Defense Technical Information Center
Compilation Part Notice

ADP013342

TITLE: Investigations on Sol-Gel Derived
Ba[0.5]Sr[0.5]Ti[1-Delta]Mn[Delta]O3 [Delta = 0.0 to 5.0 at %] Thin Films
for Phase Shifter Applications

DISTRIBUTION: Approved for public release, distribution unlimited

This paper is part of the following report:

TITLE: Materials Research Society Symposium Proceedings; Volume 720.
Materials Issues for Tunable RF and Microwave Devices III Held in San
Francisco, California on April 2-3, 2002

To order the complete compilation report, use: ADA410712

The component part is provided here to allow users access to individually authored sections
of proceedings, annals, symposia, etc. However, the component should be considered within
the context of the overall compilation report and not as a stand-alone technical report.

The following component part numbers comprise the compilation report:
ADP013342 thru ADP013370

Investigations on Sol-Gel Derived $Ba_{0.5}Sr_{0.5}Ti_{1-\delta}Mn_{\delta}O_3$ (δ = 0.0 to 5.0 at%) Thin Films for Phase Shifter Applications

R.S. Katiyar[1], M. Jain[1], S.B. Majumder[1],
R.R. Romanofsky, F.W. van Keuls, and F.A. Miranda
[1]PO Box 23343, Department of Physics, University of Puerto Rico, San Juan, PR 00931,U.S.A.
NASA, Glenn Research Center, Cleveland, OH 44135, U.S.A.

ABSTRACT

Highly (100) oriented $Ba_{0.5}Sr_{0.5}Ti_{1-\delta}Mn_{\delta}O_3$ thin films were deposited on (100) $LaAlO_3$ (LAO) substrate by sol-gel technique. We have studied systematically the effect of Mn doping on the degree of texturing, surface morphology, dielectric properties and phase transition behavior of barium strontium titanate (BST) thin films. Up to 3 at % Mn doping the degree of (100) texturing and grain size of BST (50/50) thin films were markedly improved, which led to an increased tunability from 29% (undoped) to 39% (3 at % Mn doped); measured at 1 MHz and 2.34V/µm bias field. The transition and Curie-Weiss temperatures of BST (50/50) thin films were found to be about 266 K and 185 K respectively, which confirmed the first order phase transition in the films. The variation of transition temperatures as a function of Mn doping contents in BST (50/50) thin films were influenced by the variation of stress state and surface morphology modifications induced by Mn doping. The bias field dependence of the dielectric constant and loss tangents of undoped and Mn doped films were analyzed in terms of a model based on Devonshire theory. Phase shift measurements showed that the degree of phase shift increases from 239° to 337° with 0 to 3 at% Mn doping. The insertion loss also increases from 5.4 dB (undoped) to 9.9 dB (3 at % Mn doped) with doping content so that there is no effective improvement in the κ factor, which remains in the range of 33 - 44°/dB. Modification in surface morphology and film stoichiometry induced by Mn doping is thought to play significant role in observed phase shifter characteristics.

INTRODUCTION

Modern electronic scan phase array antennas can steer transmitted and received signals without mechanically rotating the antenna. Ferroelectric phase shifters have low power requirement as compared to the ferrite based phase shifters and also, they exhibit low loss at microwave frequencies as compared to semiconductor based phase shifters. $Ba_xSr_{1-x}TiO_3$ (BST) thin films, paraelectric at room temperature (x < 0.7), are attractive candidates for tunable dielectric devices such as voltage-controlled oscillators (VCO), tunable filters, phase-shifters,

Contact author: R. S. Katiyar
email : rkatiyar@rrpac.upr.clu.edu
Tel: (787)-751-4210, Fax: (787)-764 -2571

tunable matching networks and frequency multipliers. High dielectric tunability and low dielectric loss at GHz frequencies are required for microwave applications. Moreover, for impedance matching purposes the dielectric constants of the films should be low with low leakage current densities. Fabrication of phase shifter utilizing bulk BST remains unsuccessful due to higher voltage requirement as well as higher dielectric constant. In thin film form the dielectric constant of BST is low as compared to its bulk counterpart due to finer grain size as well as presence of interfacial layers and also the dielectric can be tuned at moderate voltage compatible with modern electronic circuitry. To achieve low dielectric loss BST thin films should be grown with low defect densities and it has been reported that epitaxially grown film on lattice matched substrates has better tunability as compared to polycrystalline thin films [1]. However, epitaxially or textured thin films usually have higher leakage current densities as compared to polycrystalline thin films [2]. Efforts have been made to modify the electrical characteristics of BST thin films by adding impurity elements. Up to 1 at % Mn doping was found to increase the dielectric constant of undoped BST from 1736 to 2093, the loss tangent was reduced from 0.0153 to 0.0033 whereas the tunabilty was reduced from 66 to 63 % [3]. Mg^{2+} doping up to 5 at% in BST (60/40) thin films was found to yield single-phase perovskite thin films, however, excess Mg^{2+} addition up to 20 at% was found to yield multi-phase material [4]. The reduction of dielectric constant, loss tangent and leakage current densities with Mg doping were attractive for phase shifter application, however, the tunability of undoped BST was also found to be decreased from 28 % to 7.9 % with 20 at % Mg doping. Al^{3+} doping was found to modify the microstructure of BST (40/60) ceramics and up to 1 at % Al doping the grain size is increased and then decreased with further Al addition [5]. The dielectric constant was found to decrease with Al addition. B^{3+} doping was found useful to initiate liquid phase sintering and impart better sinterability and lower surface roughness of BST thin films. Boron was found to form highly insulating B_2O_3 layer at the grain boundary, which was claimed to be responsible for the lower leakage current densities of Boron doped BST thin films [6].

From the literature review, it appears the addition of impurity element has significant impact on the phase formation behavior, and microstructure evolution of BST thin films. In the present work we have made a systematic attempt to synthesize highly oriented Mn doped $Ba_{0.5}Sr_{0.5}Ti_{1-x}Mn_xO_3$ (x = 0.0 to 5.0 at %) thin films by an economic sol-gel process. The effect of Mn doping on the phase formation behavior, growth characteristics, surface morphology, and electrical characteristics were studied. We have fabricated eight elements coupled micro-strip phase shifters using Mn doped BST films and the quality of these films were evaluated in terms of their degree of phase shift and insertion loss characteristics.

EXPERIMENTAL METHODS

To prepare the BST precursor sol, barium and strontium acetates were co-dissolved in acetic acid and ethylene glycol. The solution was heated for complete dissolution of the precursor materials. Ti iso-propoxide was dissolved in acetic acid and the solution was added to Ba-Sr complex solution at 50°C. The sol, thus prepared was stirred for 30 minutes for complex formation and termed as parent sol. For thin film deposition, the parent sol was diluted to a concentration of $0.35ML^{-1}$ by adding acetic acid. Films were deposited by spinning the coating

sol onto clean LAO substrates at a 2500 rpm for 5s. The heating schedule of the film was decided on the basis of the thermal analysis of BaTiO$_3$ gel [7]. All films were annealed at 1050 ^{0}C for two hours. The phase formation behavior, the degree of orientation and the quality of in-plane epitaxy of the deposited films were studied using the X-ray diffraction technique. The surface morphology of the films was studied using an atomic force microscope (AFM). The low frequency (1kHz-1MHz) dielectric properties of BST thin films as a function of temperature were measured in planar electrode configuration using an impedance analyzer (HP 4294). The capacitor consists of 50 fingers that are 7 mm long, 20 im wide, and spaced 15im apart. A computer controlled thermal stage (MMR Inc.) and a thin film probe station was used to measure the temperature dependent dielectric and ferroelectric properties. The reported dielectric constant (K) was extracted from the capacitance using the conformal mapping technique originally developed by Gevorgian *et. al* [8]. Standard lift-off chemical etching technique was used to fabricate eight- element coupled micro strip phase shifters at NASA Glenn Research Center. The performance of these coupled micro-strip phase shifters at microwave frequencies were evaluated using a network analyzer (HP 8510 C, Agilent Technology).

RESULTS AND DISCUSSION

Textured growth and surface morphology of Mn-BST Films

Figure 1 shows the X-ray diffractograms of (a) undoped, (b) 1.0, (c) 3.0 and (d) 5.0 at% Mn doped BST (50/50) thin films on LAO (100) substrates. The appearance of intense (100) type diffraction peaks clearly indicates the highly (100) textured nature in all these films. The degree of (100) texture improves with Mn doping upto 3 at% as envisaged by the increased intensities of (100) type diffraction peaks and disappear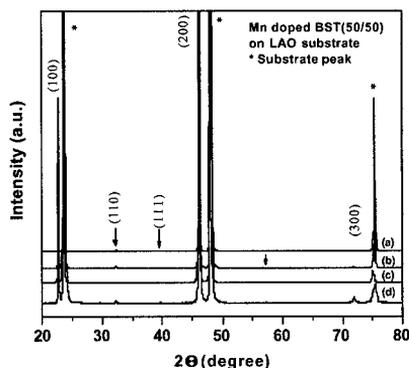ance of misaligned planes (marked by small arrows in Fig. 1(a) and (b)). With further addition of Mn, the degree of (100) texture deteriorates (Fig. 1(d)). The in-plane epitaxial quality of the Mn-doped BST thin films was analyzed by X-ray pole-figure analysis. The details of the pole-figure analysis can be found else where [9]. The pole-figure results indicate that all these films are textured in (100) direction and the degree of texturing as well as in-plane orientation improve upto 3 at% Mn doping and deteriorates with further Mn addition. Mn doping has significant influence on the surface morphology of BST (50/50) thin films. Figure 2 shows the AFM micrographs of (a) undoped, (b) 1.0 at%, (c) 3 at%, and (d) 5 at% Mn-doped BST thin films. The average grain size of these films was measured by linear intercept technique. Table I shows the variation of grain size and surface roughness of BST (50/50) with Mn doping.

Figure 1 X-ray diffractograms of (a) undoped, (b) 1.0, (c) 3.0, and (d) 5.0 at% Mn doped BST (50/50) thin films.

Table I Variation of average grain size and surface roughness with Mn doping.

Mn content (at%)	Average grain size (nm)	RMS roughness (nm)
0	141	14.3
1	152	12.1
3	252	27.5
5	213	24.2

Upto 3 at% doping content, Mn^{3+} acts as acceptor replacing Ti^{4+} at B site; and to maintain the charge neutrality oxygen vacancies are created in the lattice. The vacant lattice sites in turn increase the grain boundary mobility and therefore upto 3 at% Mn doping the grain size is increased. Beyond 3 at% Mn content, the solubility of Mn is limited in the BST lattice and probably it gets precipitated at grain boundary and thereby reduces the grain boundary mobility. This explains the smaller grain size of 5 at% film as compared to 3 at% Mn doped BST films.
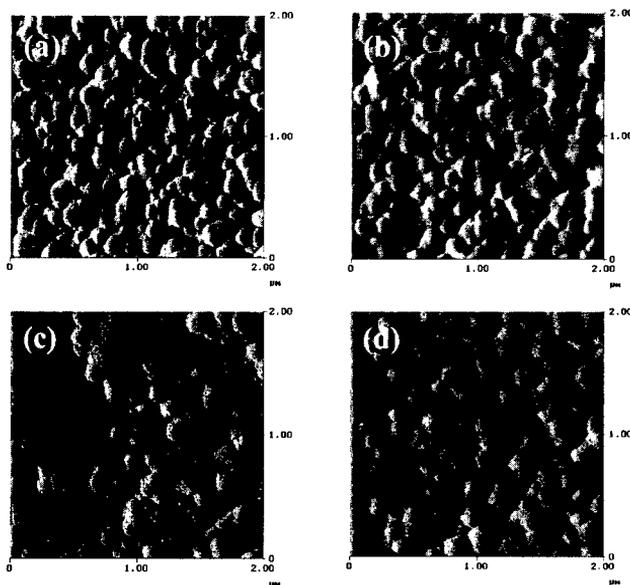

Figure 2 AFM micrographs of (a) undoped, (b) 1.0 at%, (c) 3 at%, and (d) 5.0 at% Mn doped BST thin films.

Dielectric and Leakage Current Behavior

Figure 3 shows the frequency dispersion of (a) the capacitance and (b) the loss tangent of Mn doped BST (50/50) films. The capacitance increases up to 3 at% Mn doping and then decreases with further Mn addition. The increase in capacitance could be due to the increased grain size of the BST films up to 3 at% Mn doping. Tsu *et. al.* [10] reported that since the volume of dielectric polarization is proportional to the size of the grain, the dielectric constant is

increased with the increase in grain size. As mentioned earlier, up to 3 at % Mn doping, the grain size was found to be increased in BST (50/50) thin films, which may also result in the observed increase in capacitance and thereby in dielectric constant. For the undoped and Mn doped BST (50/50) thin films, the relatively higher capacitance with low frequency dispersion indicate the absence of any low capacitance interfacial layers. The loss tangents of undoped and Mn doped films also had minimal frequency dispersion and tanδ reduces with increase in Mn
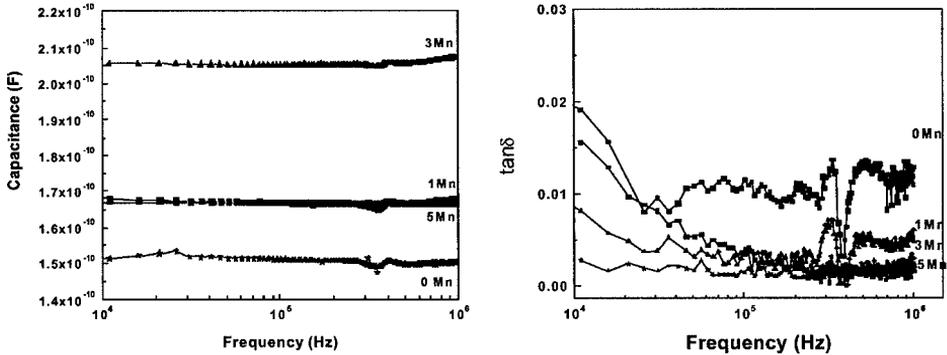

Figure 3 Frequency dispersion (a) Capacitance and (b) loss tangent of undoped and Mn doped BST thin films.

content. Mn^{+3} replaces Ti^{+4} and acts as an acceptor and thereby prevents the reduction of Ti^{+4} to Ti^{+3} by neutralizing the donor action of oxygen vacancies. Probably this reduces the loss tangent [4].

The leakage current behavior of Mn doped BST thin films were measured by measuring the current at a constant dc bias of 7 V as a function of time. The leakage current systematically increases with the increase of Mn content in BST thin films. The current (I)-voltage (V) characteristics also show similar trends (not shown). The increase of leakage current with Mn doping could be due to the fact that Mn^{3+} acts as an acceptor in BST lattice replacing Ti^{4+} and thereby creates oxygen vacancies to maintain the charge neutrality. The creation of charged vacancies in turn introduces mobile charge carriers (in this case electrons), which increase the leakage current densities.

Phase transition behavior

Figure 4 shows the temperature dependence of the measured capacitance and loss tangent of 50 fingers ID capacitor at 1MHz. The capacitance- temperature plot shows a broad maxima centered around 266K. For bulk BST (50/50) an empirical equation (T_c ($^{\circ}C$) = 371x − 241; where x is the Ba fraction) estimates the m3m-4mm (cubic to tetragonal) transition temperature to be 217.5 K [11]. The observed transition temperature of BST (50/50) thin film is thus 48 K higher than the bulk ceramics. The calculated dielectric constant is low and a broad capacitance maxima is distinguished in thin films as compared to bulk. The discrepancy between the bulk and the thin films could be due to various possible factors, which include grain size effect, non-stoichiometry, and stress. Tahan *et. al* [12] observed no maxima in the dielectric constant vs temperature curves for $Ba_xSr_{1-x}TiO_3$ (x= 0.6 to 1.0) thin films and this phenomenon was attributed to the nanoscale
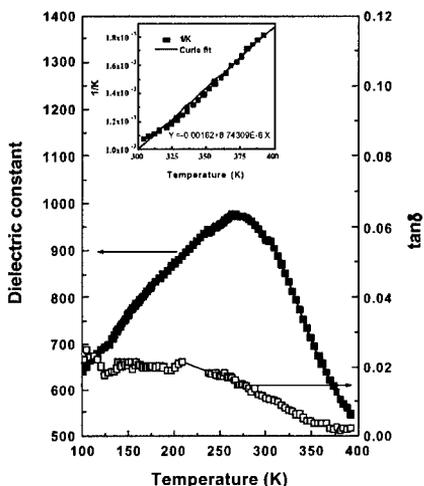
7

Figure 4 Temperature dependence of the capacitance and loss tangent of BST (50/50) thin film measured at 1 MHz. Inset shows the film follows a typical Curie-Weiss behavior in paraelectric state.

grain size of these films. As compared to bulk ceramics relatively finer grain size (R 252 nm) of undoped and Mn doped BST (50/50) thin films could be responsible for the diffuse nature of dielectric anomaly. Table II summarizes the phase transition data of undoped and Mn doped BST films. The role of Mn , in changing the transition temperature is not clearly understood. Probably Mn doping modifies the film stress state. Moreover the change in grain size with Mn doping could also be responsible for the observed variation of transition temperature. Studies are in progress to understand the reported results more clearly.

In the paraelectric state the capacitance was fitted according to the Curie-Weiss equation:

$$K = C_{Curie} / (T-\theta_c) \dots\dots\dots\dots\dots \quad (1)$$

Where, K is the dielectric constant, C_{Curie} is the Curie constant in Kelvin, T is the temperature and θ_c is the Curie temperature. Fig. 4 (inset) shows that a plot of 1/K vs T yields a straight line as predicted by equation (1) and from the linear fit the Curie constant and the Curie temperature was estimated to be 1.45×10^5 K and 185 K respectively. The fact that $\theta_c < T_m$ (where T_m is the temperature corresponding to the capacitance maxima of the K vs T plot) confirms the first order phase transition of BST films [13]. We have carried out the analysis of the observed broad dielectric behavior and the results indicate that there are more than one transitions in the films in the investigated temperature region.

Table II Summary of phase transition data of Mn-BST thin film.

Film	Dielectric constant at T_c	T_m (K)	θ_c (K)	C_{Curie} (x 10^5) (K)
Undoped BST	926	266	185	1.45
1 at % Mn-BST	846	220	108	1.6
3 at % Mn-BST	2161	255	213	2.1
5 at % Mn-BST	1149	268	150	1.7

It is known that the ionic positions and vibrations in a ferroelectric are modified by the stress, and since these changes are coupled to the polarization mechanisms in the ferroelectric, effectively the dielectric and ferroelectric properties of thin films are also affected. [14]. The effect of strain on the dielectric constant of BST thin films has recently been reported by Chang *et al* [15] based on phenomenological thermodynamic theory of bulk ferroelectrics originally developed by Devonshire [16]. Both theoretical calculation and experimental observations have verified that for tensile strain parallel to the direction of electric field vector the dielectric constant and tunability increase whereas for compressive strain they are decreased. In the present work X-ray line broadening analysis is performed to investigate the nature of strain in

annealed BST (50/50) thin film. Assuming the line broadening (β) is due to strain (e) and crystallite size (t), the following equation is used to determine the nature and magnitude of strain and crystallite size of annealed BST (50/50) film on lanthanum aluminate substrate [17].

$$\beta \cos\theta_B/\lambda = 1/t + 4e \sin\theta_B/\lambda \ \dots\dots\dots\dots\dots (2)$$

Where, β is the line width at half maximum, θ_B is the Bragg angle and λ is the X-ray wavelength. We have used (100) type of the diffraction peaks and to obtain accurate peak width at half maxima (β) and Bragg angle (θ_B), the X ray lines were fitted using two Pearson VII peaks using a commercial program (PeakFit-4, Jandel Scientific), to separate out $K_{\alpha 1}$ and $K_{\alpha 2}$ contributions and obtain the values of β and θ_B. Fig.5 shows a plot of $\beta cos\theta_B/\lambda$ vs $sin\theta_B/\lambda$. The crystallite size (t) and strain (e) estimated from the linear fit is 31 Å and +0.86% respectively. The tensile nature of the strain of the film could be due to thermal expansion mismatch or lattice mismatch between BST (50/50) film and LAO (100) substrates. The lattice parameter and thermal expansion coefficient of BST (50/50) (3.947 Å, 10.5x10^6/°C respectively) are larger than the lattice

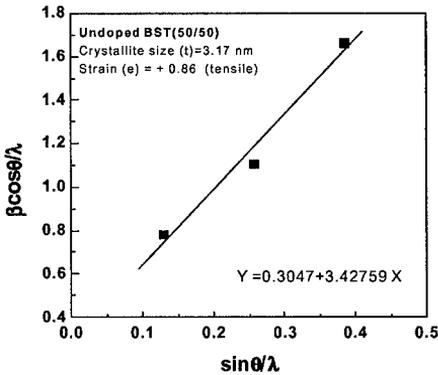parameter and thermal expansion coefficient of LAO (3.787 Å and 10x10^6/°C respectively), hence it is expected that after annealing films are under tension [15]. The shift of capacitance maxima (corresponding to the transition temperature) towards higher temperature is believed to be related to the tensile strain in the annealed BST film. As mentioned, the induced film stress arises from several contributions, eg. lattice mismatch, thermal expansion mismatch between the film and substrate. Additionally the stress field is also influenced significantly by the presence of oxygen vacancies, which alter the lattice parameter and may therefore increase, decrease or screen the overall film stress [15].

Figure 5 A plot of βcosθ/λ vs sinθ/λ of BST (50/50) thin film.

Bias field effect on dielectric properties

Fig.6 shows the room temperature frequency dispersion of capacitance and loss tangent of BST thin films measured at various sub-switching oscillation voltage levels. The increase in dielectric constant (capacitance) with the increase in oscillation voltage could be due to de-pinning of ferroelectric domain walls from the defects [18]. The increase in loss tangent with oscillation voltage also indicates that the film is not fully paraelectric at room temperature.

According to Devonshire's theory in the perovskite cubic structure, Ti ion oscillates in an anharmonic potential of the form $ar^2 + br^4$ where r is the position of the Ti ion. The Helmholtz free energy F (P,T) of the Ti ion can be expanded in even powers of the polarization P with coefficients that are a function of the temperature only; that is

$$F(P,T) = F\ (0,T) + A\ (T-\theta)P^2 + BP^4 + CP^6 \ \dots\dots \ (3)$$

Where, θ is the Curie-Weiss temperature, and A, B, C are the expansion coefficients. In the paraelectric state the free energy increases as polarization, and there is only one minimum at $P = 0$. If a small field 'E' is applied on the materials then the P^6 term can be neglected. Moreover, in the paraelectric state, where the polarization is much smaller than that in the ferroelectric state,

9

neglecting the P^6 term in the expansion of free energy is appropriate. The dielectric constant (ε_r) can be obtained by taking the second derivative of the free energy with respect to polarization. The lattice anharmonic interaction of Ti ions is responsible for the field dependence of the dielectric constant of the BST system. According to a model proposed by Johnson one can obtain a phenomenological equation that is valid in the paraelectric state [19]

$$K'/K'_o = 1 / (1 + a\,K'^3_o E^2)^{1/3} \qquad \ldots\ldots\ldots\ldots(4)$$

Where $a = 12\,B/(4\pi)^3$ is the anharmonic coefficient. Johnson also derived that the imaginary part of the relative permittivity follows another phenomenological equation

$$K''/K_o'' = 1 / (1 + a\,K'^3_o E^2)^{2/3} \qquad \ldots\ldots\ldots\ldots(5)$$

Where $(K',\ K'_o)$ and $(K'',\ K_o'')$ are the real and imaginary parts of the dielectric constant K respectively, under a field E and zero bias field respectively. Based on Eqns 4 and 5, the field variation of loss tangent $(\tan\delta_c)$ can be expressed as

$$\tan\delta_c = K''/K' = \tan\delta_{co} / (1 + a\,K'^3_o E^2)^{1/3} \qquad \ldots\ldots\ldots\ldots(6)$$

The above equations are valid only in the paraelectric state where the polarization value is negligible to that in the ferroelectric state and the applied electric field (E) is small.
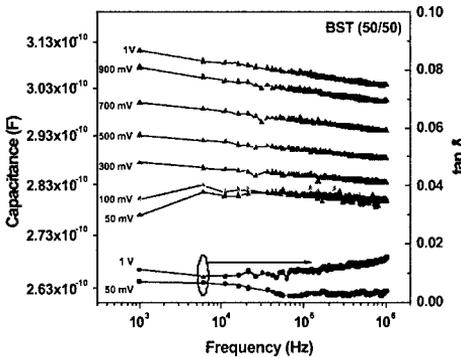

Figure 6 Room temperature frequency dispersion of capacitance and loss tangent values of BST thin film measured at different oscillation voltages.
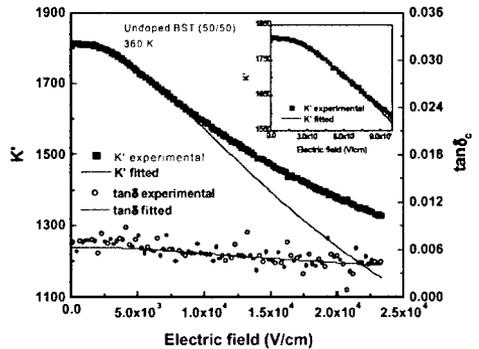
Figure 7 Bias field dependence of dielectric constant (K') and loss tangent of undoped BST film measured at 360 K applying oscillation voltage 500 mV a t 1 MHz.

Fig.7 shows the field (E) dependence of the real part of dielectric constant (K') and loss tangent $(\tan\delta_c)$ measured at 360K. The solid lines shown in the plot are obtained by curve fitting with equation (4) and (6) for K' and $\tan\delta_c$ respectively. As shown in the Figure, the theoretical plot matches well with the experimental data when the applied electric field is low (≤ 7.5kV/cm) and deviates at higher electric field. This is expected since at higher field the polarization contribution cannot be neglected and in other words eqn. 4 and 6 are not strictly valid in describing the field dependence of dielectric constant and loss tangent [20]. Similar fitting was performed to the experimental field dependence of K' and $\tan\delta_c$ at different temperatures ranging from 300 to 400 K (i.e in the paraelectric state of the film). Fig. 8 shows the temperature dependence of the anharmonic coefficient (a) and the tunability of undoped and Mn-BST (50/50) thin films. The figure shows that for undoped and Mn-doped BST (50/50) films 'a' parameter and tunability (measured at 1 MHz) and 2.33 V/μm) decrease with the increase in temperature. Note that equation (4) also indicates that tunability decreases with the decrease in 'a', K_o' or E
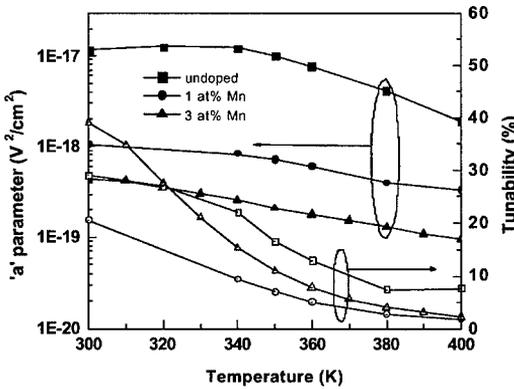
Figure 8 Temperature variation of 'a' parameter and tunability of undoped and Mn doped BST thin films.

values. The maximum tunability is obtained for 3 at% Mn-BST thin films in the vicinity of its transition temperature (~255 K) and decreases with increase in temperature. Hysteresis loop measurement of these films as a function of temperature indicates the presence of remnant polarization even at corresponding transition temperatures. The domain movement and capacitance hysteresis under dc field due to the ferroelectric nature of the film could yield unpredictable dielectric characteristics. Therefore for all practical purposes it is recommended that the working temperature for practical device s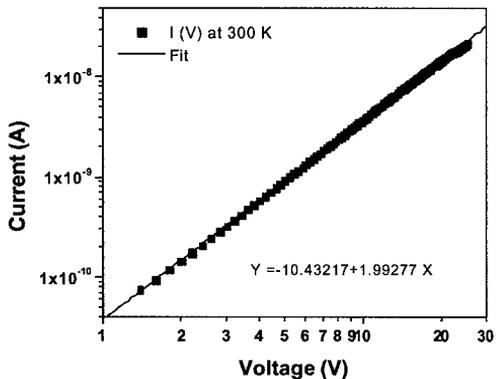lightly above the transition temperature where the hysteresis is minimized at the same time the tunability remains appreciable. It should be worthwhile to mention at this stage that Devonshire theory assumes a stress free condition. However, as mentioned earlier our film contains residual tensile stress, which could be responsible for the broadening of ferroelectric to paraelectric transition and also dilute the contribution of the anharmonic coefficient towards the tunability [20].

As shown in Fig.7 the experimental field variation of $tan\delta$ of BST film matches well with the theoretical prediction (eqn. 6) up to field strength of about 22 kV/cm. At a particular measurement frequency $tan\delta$ can be expressed as [21]

$$tan\delta = tan\delta_c + tan\delta_R \qquad \dots\dots\dots\dots (7),$$

Where $tan\delta_c$ is the intrinsic dielectric loss expressed by eqn 6 and $tan\delta_R$ is the conduction loss expressed as

$$K''/K' = 1/K' \omega RC_o \qquad \dots\dots\dots\dots (8)$$

Where ω is the angular frequency, R is the resistance and C_o is the capacitance at zero field. Figure 9 shows the current (I) –voltage (V) characteristics of BST (50/50) thin film. In this voltage range leakage current exhibits perfect linear variation confirming the ohmic nature of conduction behavior. At room temperature and also at higher temperature the calculated $tan\delta_R$ is negligible as compared to $tan\delta_c$ indicating the voltage variable capacitor loss

Figure 9 At low applied voltage the I-V characteristics of BST (50/50) thin film exhibits ohmic conduction behavior.

component ($tan\delta_c$) dominates the overall loss tangent characteristics under the applied field regime.

Phase Shifter Characteristics

A ferroelectric phase-shifter is an electric delay line, in which the amount of electrical delay, i.e. phase shift, is controlled by the dielectric constant, and hence the scan angle of a radar beam can be controlled by changing the dielectric constant of the material. We have used the highly textured undoped and Mn doped BST (50/50) films to fabricate eight element coupled micro-strip phase shifters to be used in low cost steerable antennas for communication applications.To fabricate phase shifters, the BST films were metallized with a 15 nm chromium (Cr) adhesion layer followed by a 2 im to 2.5 im thick gold (Au) film using the electron beam evaporation at NASA Glenn Research Center. Standard lift-off chemical etching techniques were used to fabricate the Au/BST/LAO phase shifters. Finally, a Cr/Au ground plate with the same thickness were e -beam evaporated on the back of the substrate. The performance of these coupled micro-strip phase shifters at microwave frequencies was evaluated by measuring the transmission (S_{21}) scattering parameters between 14 to 17 GHz using an HP 8510C network analyzer. All loss measurements quoted here include the losses due to the SMA launchers, which are estimated to be 0.25 to 0.5 dB. The measurements were taken in vacuum to avoid the dielectric breakdown in the air under high dc fields between coupled micro-strip sections.

The degree of phase shift and insertion loss (in the frequency range of 13.5 to 15 GHz) of undoped and Mn doped BST (50/50) thin films as a function of bias voltage are shown in Fig. 10. The phase shift increases systematically from 239° (undoped) to 337° (3 at% Mn doping) and decrease with further Mn addition The degree of phase shifts, insertion losses and the figure of merits (κ, defined by the ratio of phase shift /insertion loss) for undoped and Mn doped BST (50/50) films are tabulated in Table III. As shown in the table, although there is a significant improvement of the degree of phase shift up to 3 at % Mn doping, the insertion loss also increases (5.4 - 9.9 dB) with the increase in dopant concentration and as a result the effective κ factor does not improve significantly and remains in the range of 33 – 44 °/dB. The improvement of the degree of phase shift could be due to either the increased grain size or the improvement of
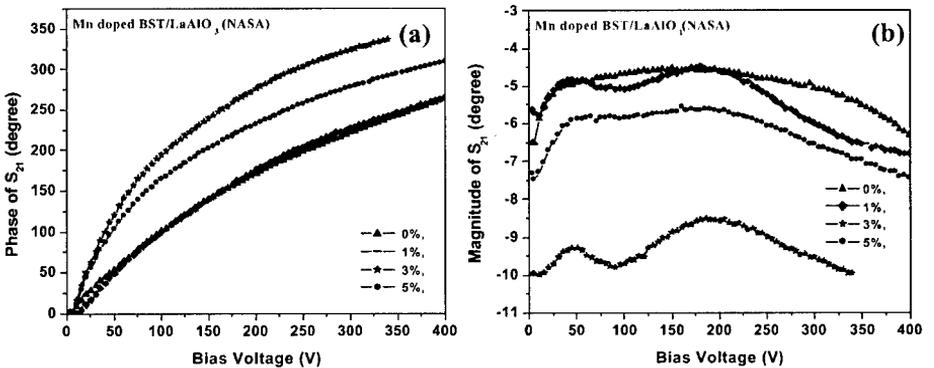

Figure 10 Variation of (a) Phase shift, and (b) insertion loss, for undoped and Mn doped BST films as a function of bias voltage.

(100) texturing up to 3 at % Mn doping. As mentioned earlier the surface roughness also increases with the increase in Mn content up to 3 at %. The higher insertion loss with the increase in Mn content could be either due to higher surface roughness or creation of oxygen vacancies due to the acceptor nature of Mn doping in BST lattice.

Table III Phase shifter characteristics of Mn doped BST (50/50) thin films measured at 16 GHz and at 339 Volts.

Film composition	Phase shift (^{o})	Insertion loss (dB)	κ factor (^{o}/dB)
Undoped BST (50/50)	239	5.4	44
1Mn-BST	242	6.5	37
3Mn-BST	337	9.9	34
5Mn-BST	291	6.9	42

CONCLUSIONS

Highly (100) oriented undoped and Mn doped BST (50/50) thin films were successfully grown on LAO (100) substrates by sol-gel technique. Our results demonstrated that Mn doping has a strong influence on the growth characteristics; microstructure and electrical properties of BST (50/50) thin films. Up to 5 at % Mn doping BST (50/50) thin films crystallize into single-phase perovskite structure. The degree of (100) texturing improves up to 3 at % Mn doping. Pole-figure analysis shows the improvement of in-plane epitaxy upto 3 at % Mn doping. The grain size increases up to 3 at % Mn doping, however the surface roughness also increases with the grain growth. From the dielectric measurements we found that the dielectric constant of the BST (50/50) film increases up to 3 at % Mn doping, maintaining low dielectric loss values ($\tan\delta$ $\sim10^{-2}$). We have fabricated eight element coupled micro-strip phase-shifters (CMPS) and tested them in terms of their degree of phase shift and insertion loss characteristics. Phase shift measurements showed the maximum tunability increases from 239° to 337° with 0 to 3 at% Mn doping however, the insertion loss also increases (~5.4 dB (undoped) to 9.9 dB (3at % Mn doped)) with the increase with doping content so that there is no effective improvement in the κ factor which remains in the range of 33 – 44°/dB. The improvement in degree of phase shift in case of 3 at % Mn doped BST (50/50) film is attractive for phase shifter application. However the insertion loss should be minimized for practical device applications. The relatively higher insertion loss in 3 at% Mn doped films could be due to its rougher surface morphology. Further research is in progress to further optimize the process parameters to grow dense and smoother Mn doped BST (50/50) films with reduced insertion loss and higher κ factor.

REFERENCES

1. D. Dimos and C.H. Muller, *Ann. Rev. Mater. Sci.,* **28**, 397 (1998).
2. K. Abe and S. Komatsu, *Jpn. J. Appl. Phys.,* **32**, 4186 (1993).
3. H. D. Wu and F. S. Barnes, *Integrated Ferroelectrics,* **22**, 291 (1998).
4. M. W. Cole, P. C. Joshi, M. H. Ervin, M. C. Wood, and R. L. Pfeffer, *Thin Solid Films,* **374**, 34 (2000).
5. L. Wu, Y. C. Chen, Y. P. Chou, Y. T. Tsai, and S. Y. Chu, *Jpn J. Appl. Phys.,* **38**, 5154 (1999).
6. S.I. Jang, H.M. Jang, *Thin Solid Films,* **330**, 89 (1998).
7. S.B. Majumder, M. Jain, A. Martinez, R.S. Katiyar, F.W. van Kuels, and F.A. Miranda, *J. Appl. Phys.,* **90**, 896 (2001).
8. S. Gevorgian, E. Carlsson, S. Rudner, L. D. Wernlund, X. Wang, and U. Helwersson, *IEEE Proc. Microm. Antennas Propag.,* **143**, 397 (1996).
9. M. Jain, S.B. Majumder, A. Martinez, R.S. Katiyar, F.W. van Kuels, R.R. Ramanofsky, and F.A. Miranda, *Integrated Ferroelectrics,* **42**, 207 (2002).
10. R. Tsu, H.Y. Liu, W. Y. Hsu, S. Summerfelt, K. Aoki, and B. Gnade, *Mat. Res. Soc. Symp. Pro.,* **361**, 275 (1995).
11. B. Jaffe, W.R. Cook Jr, and H. Jaffe, *Piezoelectric Ceramics,* (R.A.N Publishers, Marietta, OH, 1991).
12. D.M. Tahan, A. Safari, L.C. Klein, *J. Am. Ceram. Soc.,* **79**, 1593 (1996).
13. Y. Xu., *Ferroelectric Materials and Their Applications,* (Elsevier Science Publishers B.V., NY 1991).
14. W. Chang, C.M. Gilmore, W.J. Kim, J.F. Pond, S.W. Kirchoefer, S.B. Qadri, D.B. Chrisey, and J.S. Horwitz, *J. Appl. Phys.* **87**, 3044, (2000).
15. W. Chang, J.S. Horwitz, A.C. Carter, J.M. Pond, S.W. Kirchoefer, C.M. Gilmore, and D.B. Chrisey, *Appl. Phys. Lett.,* **74**, 1033 (1999).
16. A.F. Devonshire, *Philos Mag.* **42**, 1065 (1951).
17. W.H. Hall, *Proc. Phys. Soc.* **62**, 741, (1949).
18. Dragan Damjanovi,*Rep. Prog. Phys.* **61** (9), 1267 (1998).
19. K.M. Johnson, *J. Appl. Phys,* **33**, 2826 (1962).
20. J.W. Liou and B.S. Chiou, *J. Am. Ceram. Soc.,* **80**, 3093 (1997); J.F. Scott, *Ferroelectric Review,* 1, 1 (1998).
21. L. Wu, Y.C. Chen, Y.P. Chou, Y. Tsai, and S.Y. Chu, *Jpn. J. Appl. Phys.,* **38**, 5154 (1999).